Main Group Chemistry 15 (2016) 231–242
DOI 10.3233/MGC-160202
IOS Press

The synthesis, characterization and phase stability of tin sulfides (SnS_2, SnS and Sn_2S_3) films deposited by ultrasonic spray

Imen Bouhaf Kherchachi*, Abdallah Attaf, Hanane Saidi, Adel bouhdjar, Hamza bendjdidi, Benkhetta Youcef and Rahil Azizi
Physic Laboratory of Thin Films and Applications LPCMA, University of Biskra, Biskra, Algeria

Abstract. In this study, we will deal with the influences of deposition time on structural, optical and electrical properties of Sn_xS_y films which have grown through ultrasonic spray technique. The Sn_xS_y thin films are deposited on glass substrate at 300°C with a deposition time of $t = 2$ min-10 min, using two precursors: tin (II) chloride and tin (IV) chloride, respectively. The obtained films were characterized by X-ray diffraction (XRD), The UV–VIS–NIR optical transmittance measurements and the electrical resistivity by four -points. The X-ray diffraction (XRD) analysis of Sn_xS_y films indicates three phases of SnS_2, SnS and Sn_2S_3 phases crystallites. In addition, this analysis revealed that SnS_2 phase stability is superior than SnS and Sn_2S_3 stability. The results of (UV) spectroscopy visible spectrum demonstrate that films deposited at 10 min are low transmittance in the visible region for two precursors, and a direct band gap found to decrease with increase in deposition time. Electrical measurements indicate that the resistivity behavior depends on the used precursors and deposition time.

Keywords: Sn_xS_y thin films, stability, tin sulfide, ultrasonic spray, deposition time, precursors

1. Introduction

Searching for thin film materials for solar energy conversion and other related applications has been recently identified. Compared to other studies, using metal chalcogenides,as a class of materials, had shown somewhat superior performance [1]. Among the new materials that have attracted considerable attention in the binary is composed of tin sulfide due to its interesting physico-chemical properties, and which could also replace other material such as quaternary $CuInGaSe_2$ in photovoltaics and thus avoid selenium which is toxic [2–4]. In the phase diagram of the Sn–S binary system, there are three stoichiometric known components, with different tin to sulfide ratios: SnS, Sn_2S_3 and SnS_2 [5–7]. From a technological standpoint, tin mono-sulfide (SnS), the tin disulfide (SnS_2) and the compound of Sn_2S_3 are among the most interesting [8–10] materials. In addition, there are many advantages of these later in the use of photovoltaic applications such as the gap that can approach the optimum for the conversion of solar energy (1.50 eV) [11, 12], low cost, non-natural toxic and easily developed

*Corresponding author: Imen Bouhaf Kherchachi, Physic Laboratory of Thin Films and Applications LPCMA, University of Biskra, BP 145 RP, 07000 Biskra, Algeria. Tel.: +213795118708; E-mail: imenphy12@gmail.com.

ISSN 1024-1221/16/$35.00

because these components are very abundant on earth [13]. Tin disulfide (SnS_2) is a semiconductor with Cdl_2 type structure [14]. It is a good light absorber (absorption coefficient of 10^4 cm^{-1}) with varying band gap energy (0.8–2.88 eV) [15–17]. Several deposition techniques have been used to prepare tin sulfide thin films, including: chemical bath deposition method (CBD) [18], thermal evaporation [19], RF sputtering [20], electrochemical deposition [21, 22], hot wall method [23], novel hydrothermal method [24], successive ionic layer adsorption and reaction method (SILAR) [25, 26], pulse electrodeposition method [27], spray pyrolysis [28, 29], electron beam evaporation [3], plasma-enhanced chemical vapor deposition (PECVD) [30], and dip coating method [14].

The review of literature had proved that the influence of nature of precursors with deposition time on structural, optical and electrical properties of Sn_xS_y thin films deposited by ultrasonic spray has not been previously examined. But, it is important to control these properties of Sn_xS_y films for determining the experimental conditions for photovoltaic applications. Hence, in this paper, we have aimed to find out how deposition time and the two precursors affect the structural, optical and electrical properties of Sn_xS_y thin films obtained by ultrasonic spray method.

2. Experimental procedure

2.1. Preparation of spray solution

In our experiment, Sn_xS_y thin films are prepared using a homemade ultrasonic spray deposition system. The precursors used as sources of tin (Sn) are: ($SnCl_2$: $2H_2O$), ($SnCl_4$: $5H_2O$), whereas the precursor used for sulfide (S) is the thiourea ($SC(NH_2)_2$). Two initial types of solutions were prepared and will be referred to as solution 1 and solution 2 and the films that were obtained from them will be referred to as films 1 and films 2 respectively. In solution 1 and solution 2 molarity of sufide (M_{Sn}) was 0.05 mol/l and the molarity of thiourea (M_S) was 0.1 mol/l both of them were dissolved in methanol. The substrate temperature was 300°C, the solution flow rate was 50 ml/ h, the distance between nozzle and substrate was 5 cm all of them were kept constant. However, the spraying deposition time varied from 2 to 10 min.

2.2. Characterization

The films were characterized by means of structural optical and electrical techniques. The X-ray diffraction studies were carried out using a D8 ADVANCED BRUKER diffractometer with copper anode having a wavelength $\lambda = 1.5418A^{\circ}$. The UV–VIS–NIR transmittance measurements were performed UV-VIS-NIR (UVI-3101 PC SHIMADZU) Spectrometer has been used in the range 300–900 nm for the calculations for the transmittance. The electrical resistivity of films was measured by four-point.

3. Results and discussion

3.1. Thickness calculation

After deposition, the thin film thickness (e) was evaluated using the weight difference method with the following relation [31]:

$$e = \frac{m}{\rho.\mathrm{A}} \tag{1}$$

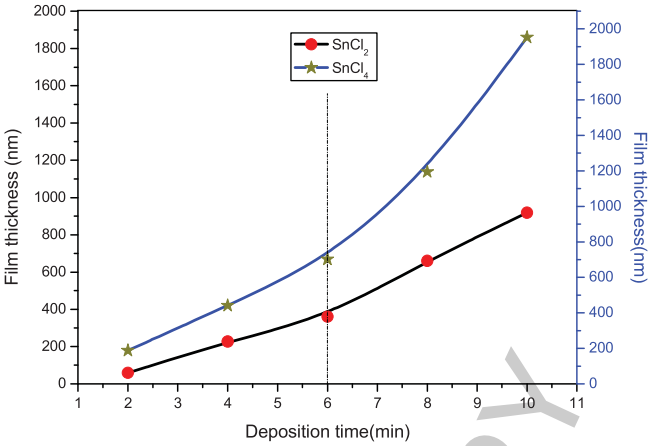

Fig. 1. The Variation of film thickness as a function of deposition time.

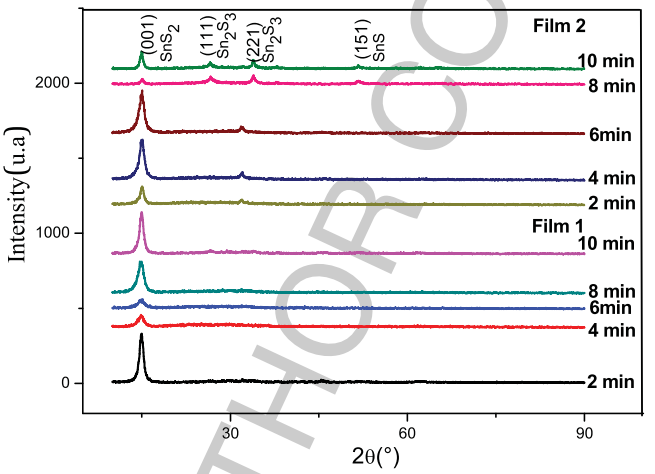

Fig. 2. XRD diffraction pattern of the two deposited films 1 and 2. SnS_2, Sn_2S_3, SnS.

where m is the mass of the film deposited on the substrate, ρ is the density of the deposited material in the bulk form and A (in cm^2) is the effective area on which the film was deposited.

Figure 1 shows the evolution of the films thickness with the deposition time for two films. As can be seen, at low deposition time 2 min the films thickness for two films is small, this indicates that the nucleation step is very short for two films, after 4 min the films thickness increases linearly with the deposition time. As well as the value of film thickness 2 is greater than the value of film thickness 1.

3.2. Structural studies

The X-ray diffraction patterns of both types of films are shown in Fig. 2. For the films 1, it can be noticed that the films which are formed at 2 to 6 min show a peak corresponding to SnS_2 hexagonal phase [32] (JCPDS card No 23-0677) with preferential orientation in the plane (001) around the angle $2\theta = 15.02^\circ$. The films grown at 8 to 10 min and the previous one (2 to 6 min) show the same prominent peak corresponding to SnS_2 whereas other peaks observed at 8 min of 2θ values of 26.70°, 33.98° and 50.27° were found to match with reflections of minimum intensity from (111), (221) and (110) crystallographic planes of Sn_2S_3 and SnS_2 phase respectively. The peak seen at 10 min of 2θ values

of 45.56° is found with reflections from (002) plane of SnS phase (JCPDS card No 390354), For the films 2, it can be noted that the XRD patterns of the thin films at (2–6 min) show peaks corresponding to SnS_2 hexagonal phase [32] with preferential from (001) plane and other peak of minimum intensity corresponding to SnS phase with orthorhombic in structure from (040) plane [33]. Moreover, the figure bellow displays the intensity of the peak (001) decrease with increasing deposition time, in contrary for the intensity of the peak (040) correspondent SnS phase. Hence, with rising deposition time, the analysis of the XRD pattern of film deposited after 6 min indicates the formation of SnS_2, Sn_2S_3 and SnS phase with other orientations (001), (111), (221) and (151). Similar results about the formation of SnS_2 phase by spray pyrolysis technique using $SnCl_2$: $2H_2O$ and $SnCl_4$: $5H_2O$ precursor has been observed by several studies [34–36]. Also the same observation by other groups using other deposition techniques [14, 37, 38]. But the difference between their work and our work is the appearance of the new phase.

The appearance of phase SnS in the film 2 at the first deposition time 2 min can be referred to the solubility of the solution or the energy of bindings between the atoms in both solutions. Solubility in solution 2 is bigger than the solubility of solution 1, for that solution 2 produces a wide number of Sn atoms. Atoms Sn leads to two significant results: the formation of SnS and SnS_2 phases and the emergence of a third new phase called Sn_2S_3 at deposition time 8 min. The former phase appeared of big intensity at XRD analysis in the films 2 when compared to films 1. As a result, on the one hand the appearance of Sn_2S_3 at 8 min its intensity decreases at 10 min and on the other hand intensity of the SnS_2 phase decreases. Consequently, Sn_2S_3phase stability is inferior than SnS and SnS_2 stability.

A prominent (001) peak for two precursors indicates that the crystallite structure of the films is oriented with their c-axis perpendicular to the substrate plane, due to its surface energy and that the atoms will arrange themselves into the plane with the lowest surface energy [39, 40]. Thus, it can be deduced that the main effect on the chemical composition is caused by the precursor nature and by the deposition time. The use of both solutions 1and 2 have proved that (001) reffered to as SnS_2 phase is the preferred orientation in all deposition times. Whereas, SnS and Sn_2S_3 phases appeared only when using $SnCl_4$ at large deposition times 8 and 10 min.

3.2.1. Texture coefficient, crystallites size, strain, dislocation density and lattice parameters

The preferential orientation of the dominant phase of the sample has been determined by means of the texture coefficient (TC) using the expression [41]:

$$TC(hkl) = \frac{I(hkl)/I_0(hkl)}{\frac{1}{N}\sum_n I(hkl)/I_0(hkl)} \tag{2}$$

Where I_0 (h k l) is the standard intensity of the (h k l) plane, I (h k l) is the observed intensity of the (h k l) plane and N is the reflection number and n is the number of diffraction peaks. Results were presented in Table 1. From the results of the texture coefficient calculations, it was found that preferential orientation of deposited films with different deposition time of 2,4,6,8 and 10 min for two precursors was the (001) orientation. Figure 3 shows the variation of TC (001) for two films. As seen, for films 1 the value of TC (001) between 2–6 min takes average constant value and then increasing with increase in deposition time. Whereas, TC of film 2 increasing when deposition time varied from 2–6 min and then decreased rapidly with increase in deposition time. The minimum value noticed at 8 min.

The mean crystallite size D was calculated from the most intense peak of the different present phases in the samples using Debye–Scherrer's formula [25, 42]:

$$D = \frac{(0.9.\lambda)}{\beta.\cos\theta_{hkl}} \tag{3}$$

Table 1
Structural parameters of spray ultrasonic Sn_xS_y film

Deposition time (min)	Films 1			Films 2			Lattice Parameters (Å) according to JCPDS card number 23-0677
	h k l planes	Lattice Parameters (Å)	TC	h k l planes	Lattice Parameters (Å)	TC	
2	(001)	$a = 3{,}638$	1	(001)	$a = 3.582$	1.21	
		c = 5,932		(040)	$c = 5.840$	0.78	
4	(001)	$a = 3{,}533$	1	(001)	$a = 3.600$	1.44	Hexagonal
		c = 5,760		(040)	$c = 5.869$	0.56	structure
6	(001)	$a = 3{,}636$	1	(001)	$a = 3.603$	1.41	$a = 3.648$
		c = 5,927		(040)	$c = 5.873$	0.59	$c = 5.899$
8	(001)	$a = 3{,}630$	1.04	(001)	$a = 3.592$	0.073	
	(111)	c = 5,917	0.72	(111)	$c = 5.856$	0.83	
	(221)		2.04	(221)		2.91	
	(110)		0.18	(151)		0.17	
10	(001)	$a = 3{,}638$	2.01	(001)	$a = 3.635$	0.23	
	(111)	c = 5,931	0.73	(111)	$c = 5.925$	0.76	
	(002)		0.24	(221)		2.83	
				(151)		0.14	

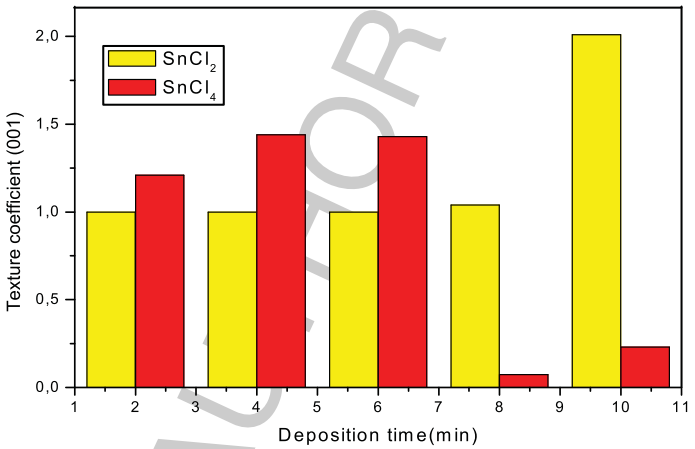

Fig. 3. The variation of preferential orientation as a function of deposition time for (001) plane.

Where D, λ, β and θ_{hkl} are the crystallite size, the wavelength, the full width at half maximum (FWHM) and the Bragg angle of the main peak of the obtained XRD spectrum, respectively. Figure 4 shows the variation of the crystallite size as a function of the deposition time. The values of crystallite size are comparable to those reported by other research [14, 43]. We can divide the figure into 2 ranges:

- The range (I):2–6 min: We found that the values of crystallite size are nearly the same either using precursor 1 or 2.
- The range (II):6–10 min: The crystallite size increase when using precursor 2 and decrease when using precursor 1 this can be referred to existence of Sn atoms in solution 2 which leads to the easy break down of bindings between Sn and Cl and all of this is supported in Fig. 2 that indicate the appearance of other phases. Also the concentration of the defect (grain boundary) is low in the films 2 in contrast with films 1.

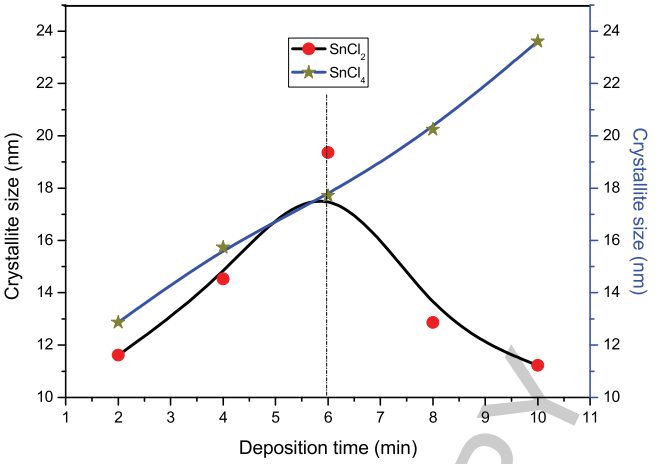

Fig. 4. The variation of the grain size for the two series with the deposition time.

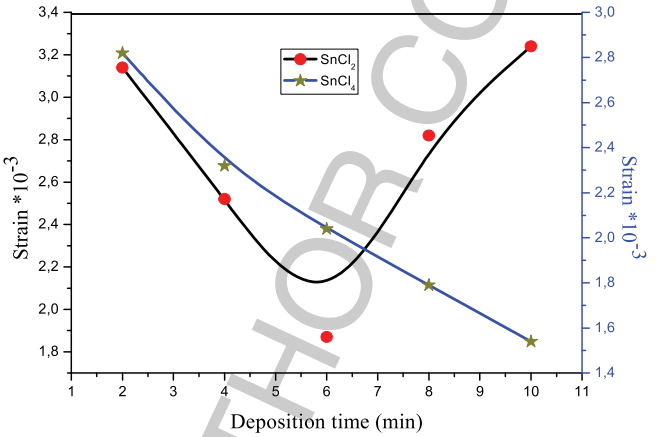

Fig. 5. The variation of strain ε in the films network as a function of the deposition time.

The strain ε in the films is evaluated using the following formula [44]:

$$\varepsilon = \frac{\beta . \cos\theta}{4} \tag{4}$$

Figure 5 shows the variation of ε versus the deposition time. Comparatively with the variation of the crystallite size D, the internal strain behavior of the two films 1 and 2 follows an opposite trend of D. This comportment is due to the fact that grains growth is controlled by the strain in film network. Because the presence of internal strain in the film network cause a minimization in the grain growth driving forces, which prevent the grain size enlargement during the film formation [2, 45]. Similar behavior has been observed on SnS films deposited with Chemical bath at increasing deposition time [46].

Using crystallite size values, the dislocation density (δ), defined as the length of dislocation lines per unit volume of the crystal has been calculated by using the Williamson and Smallman's formula [47]:

$$\delta = \frac{1}{D^2} \tag{5}$$

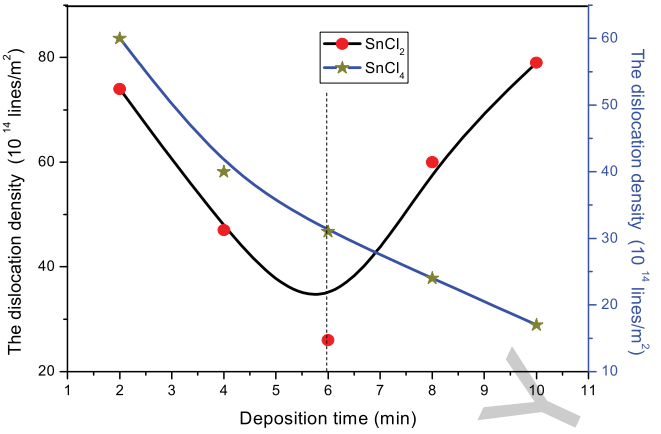

Fig. 6. The variation of the dislocation density with deposition time.

Figure 6 represents the variation of dislocation density with deposition time for two precursors. It is clearly observed that in the film 1 the dislocation density is found to decrease while increasing deposition time from 2 to 6 min, after that it increases while the dislocation density decreases of the film 2. It is clearly observable that there is an inter relationship between: crystallite size, strain and dislocation density. While there are increasing variations in the crystallite size, there are decreasing variations in the strain and dislocation density. Similarly this result has been achieved by another researcher [48].

The lattice parameters a and c for hexagonal phase structure can be determined by the relation Equation (6) [26]:

$$\frac{1}{d_{hkl}^2} = \frac{4}{3}\left(\frac{h^2 + kh + k^2}{a^2}\right) + \frac{l^2}{c^2} \tag{6}$$

The lattice parameters of the dominate phase in films 1 and 2 were obtained comparing the XRD pattern of Fig. 2 with the data reported in the JCPDS card that was mentioned earlier in this report. And according to the ASTM card number 23-0677, the lattice constants are in good agreement with the reported value.

3.3. The optical studies

The optical transmittance with wavelength of tin sulfide films Sn_xS_y was measured in wavelength range of 300–800 nm. The transmission spectra in deposited time range of 2–10 min are shown in Fig. 7. What can be noticed from the previous figure is that the transmittance of film varied from 57.22–8.338% and from 55.22 –14.25% for two films respectively. The optical transmittance for the film that has been prepared at 8 min using solution 2 was almost between the transmittance of film deposited at 4 min and 6 min that lead to the appearance of the Sn_2S_3 phase which results in low disorganized reduce of transmittance but the small intensity of the later in film 1 exhibits a well decreasing of transmittance. Through the observation of Fig. 7 we can see that there is an interference fringes at 2, 4 and 6 min when using the solution 2 indicates that the texture appeared smoothly.

The optical band gap of films is estimated from Tauc relation [43]

$$(\alpha h\upsilon) = A(h\upsilon - E_g)^n \tag{7}$$

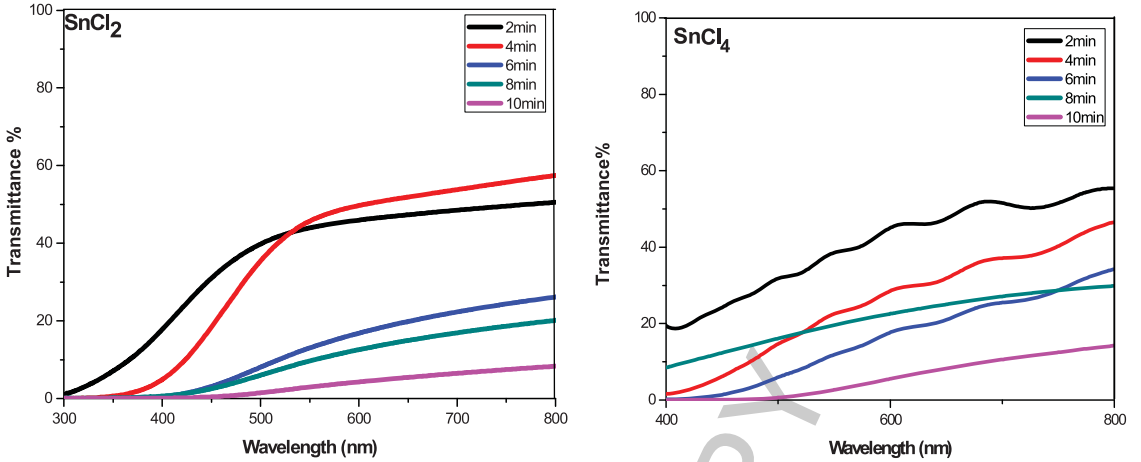

Fig. 7. Transmission curves for Sn_xS_y at different deposition time.

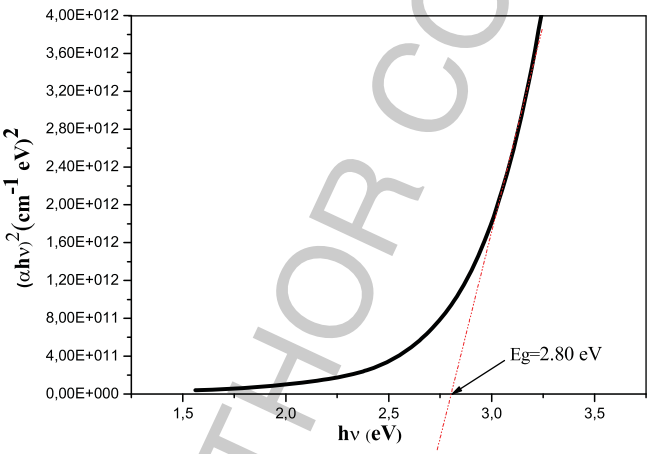

Fig. 8. The plot of $(\alpha h\nu)^2$ vs. $(h\nu)$ for Sn_xS_y film.

Where α is absorption coefficient, A is the constant independent of photon energy (hν), h is the Planck constant and E_g is the optical band gap of the material and the exponent $n = 1/2$ stands for the allowed direct transitions. On the other hand, we have used the Urbach energy (E_u), which is related to the disorder in the film network, as it is expressed follow [49]:

$$A = A_0 \exp\left(\frac{h\upsilon}{E_u}\right) \tag{8}$$

where A_0 is a constant $h\nu$ is the photon energy and E_u is the Urbach energy. In Fig. 9, for two films, the band gap decreases with increasing deposition time. Similar values of optical band gap have been found by other researchers [50, 51]. According to these data, SnS_2 and the mixture of SnS_2 with Sn_2S_3 have greater value of the band gap energy than SnS as stated by other authors [52]. The decrease in optical band gap can be due to increase the film thickness with increase in deposition time, they have also observed decrease in the optical band gap of SnS thin films with increasing of film thickness [53]. The difference in optical band gap between using solution 1 and solution 2 in addition to the previous results it appears that there is a strong decreasing in gap which can arrives 2.6 eV for film 2 in comparatively to film 1 (Fig. 9). Finally, we can conclude that $SnCl_4$ produces films in the deposition

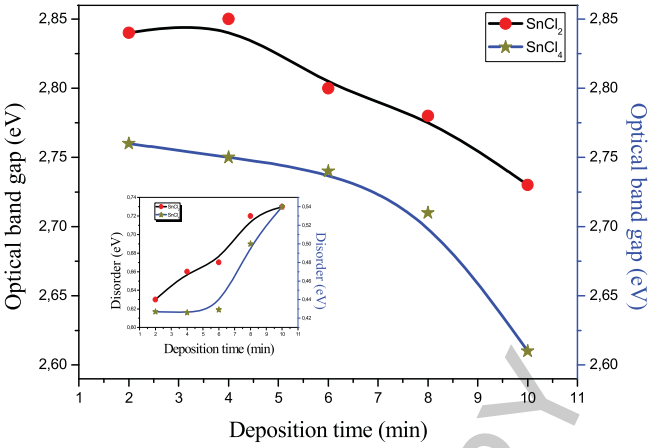

Fig. 9. The variation of band gap energy and disorder of Sn_xS_y at different deposition time.

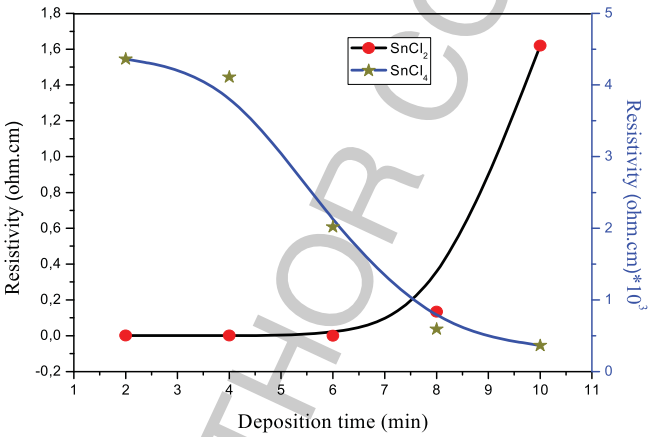

Fig. 10. Electrical resistivity of Sn_xS_y thin films.

time 6–10 min more that are useful as absorbent film in solar cells in contrast with the prepared films in the same range of deposition time using $SnCl_2$. The urbach energy varies inversely of band gap. The same observation has been found by other researcher [54].

3.4. Electrical studies

In Fig. 10, we can notice that when the deposition time between 2–6 min has no effect of the resistivity for the films 1 then after 6 min a slight increasing can be caused by smaller grain size (see Fig. 4). Similar interpretations were obtained by E. Guneri et al. in SnS thin films deposited by chemical bath deposition at different deposition time [55]. But the resistivity of films 2 decreasing in all deposition time from 2 to 10 min and the low resistivity appeared in the films deposited at 10 min which deduces that it is the appropriate film for the fabrication of solar cells. Similar value of resistivity has been found by Shuying Cheng et al. [27]. In addition, for the films 2 can be interpreted the decreases of resistivity by the increase of the crystalline size with increasing deposition time. The same variation of the resistivity has been observed by J. H. Lee et al. [56] and N. Koteeswara Reddy et al. [35].

4. Conclusions

In summary, we can say that in this study we have proved that the deposition time and the precursor both affect the thin films (1 and 2) and provide us with different behaviors and interesting characteristics. X-ray diffraction reveals a good crystalline structure with (001) orientation which corresponds to SnS_2 phase and another phase SnS appeared of films 2 starting from 2 min while at film 1 it appeares only when the film is deposited at 10 min. For both films, the optical and electrical tests show that the transmittance and resistivity decreasing with increases the deposition time. Finally, we conclude that the film 2 produces better results from structural, optical and electrical proprieties compared to the films 1. In addition, the deposition time has effects on these properties in which we can notice that there is two range from 2 to 6 min and 6 to10 min. This later supplies better results that appears through: the crystallite size, optical band gap and resistivity for the film prepared using solution 2 compared to the film prepared using solution 1, whereas the film deposited at 10 min that is characterized (D = 23.61 nm, T = 14.25%, E_g = 2.61 ev and $\rho = 0.36 \times 10^3 \Omega$.cm) is an optimal value and it is preferred in the use of photovoltaic applications.

References

[1] N.K.H. Abriksov, V.F. Bankia, L.V. Poretskaya, L.E. Shelimova and E.V. Skudnova, Semiconducting II-VI, IV-VI and V-VI compounds. Plenum 1969.

[2] B.G. Jeyaprakash, R. Ashok kumar, K. Kesavan and A. Amalarani, structural and optical characterization of spray deposited SnS thin film, *J American Science* **6** (2010), 3.

[3] A. Tanussevski and D. Poelman, Optical and photoconductive properties of SnS thin films prepared by electron beam evaporation, *J Solar Energy Materials and Solar Cells* **80** (2003), 297–303.

[4] Z. Zainal and S. Nagalingam, *J Materials Science: Materials in Electronics* **16** (2005), 281–285.

[5] L. Burton, D. Colombara, R. Abellon, F. Grozema, L. Peter and T. Savenije, Synthesis, characterization, and electronic structure of single-srystal c, and SnS_2, *J Chem Mater* **25** (2013), 4908.

[6] L.S. Price, I.P. Parkin, A.M.E. Hardy and R.J.H. Clark, Atmospheric pressure chemical vapor deposition of tin sulfides (SnS, Sn_2S_3, and SnS_2) on glass, *J Chem Mater* **11** (1999), 1792.

[7] L.A. Burton and A. Walsh, Phase stability of the earth-abundant tin sulfides SnS, SnS_2, and Sn_2S_3, *J Phys Chem C* **116** (2012), 24262.

[8] T. Chattopadhyay, A. Werner and H.G. von Schnering, Temperature and pressure induced phase transition in IV-VI compounds, *J Review Phys Appl* **19** (1984), 807–813.

[9] H. Wiedemeier, H.G. Von Schnering and Z. Krist, **148** (1978), 295.

[10] R.W.G. Wyckoff, Crystal Structure (John Wiley), **1** (1963), 89.

[11] C. Gao, H. Shen and L. Sun, Preparation and properties of zinc blende and orthorhombic SnS films by chemical bath deposition, *J Applied Surface Science* **257** (2011), 6750–6755.

[12] J. Yang, Q. Tian, Z. Chen, X. Xu and L. Zha, Synthesis and characterization of tin disulfide hexagonal nanoflakes via solvothermal decomposition, *J Materials Letters* **67** (2012), 32–34.

[13] C. Yang, W. Wang, Z. Shan and F. Huang, Preparation and photocatalytic activity of high-efficiency visible-light-responsive photocatalyst SnSx/TiO2, *J of Solid State Chemistry*, **182** (2009), 807–812.

[14] S.K. Panda, A. Antonakos, E. Liarokapis, S. Bhattzcharya and S. Chaudhuri, Optical properties of nanocrystalline SnS_2 thin films, *J Mat Res Bull* **42** (2007), 576.

[15] S. Acharya and O.N. Srivastava, Electronic behaviour of SnS_2 crystals, *J Phys Status Solidi* **65** (1981), 717–723.

[16] G. Domingo, R.S. Itoga and C.R. Kannewurf, Fundamental optical absorption in SnS_2 and $SnSe_2$, *J Phys Rev* **143** (1966), 536–541.

[17] B. Thangaraju and P Kaliannan, Spray pyrolytic deposition and characterization of SnS and SnS_2 thin films, *J Phys D Appl Phys* **33** (2000), 1054–1059.

[18] A.J. Ragina, K.C. Preetha, K.V. Murali, K. Deepa, T.L. and J. Remadevi, Wet chemical synthesis and characterization of tin sulphide thin films from different host solutions, *J Advances in Applied Science Research* **2** (2011), 438–444.

[19] P. Jain and P. Arun. Parameters influencing the optical properties of SnS thin films, *J of Semiconductors* **34** (2013), 9.

[20] K. Hartman, J. Johnson, M. Bertoni, D. Recht and M.J. Aziz, SnS thin-films by RF sputtering at room temperature *J Thin Solid Films*, **519** (2011), 7421–7424.

[21] R. Mariappan, T. Mahalingam and V. Ponnuswamy, Preparation and characterization of electrodeposited SnS thin films, *J Optik* **122** (2011), 2216–2219.
[22] M.M. Kamel and M.M. Ibrahim. Electrochemical deposition and characterization of SnS thin films, *J Solid State Electrochem* **15** (2011), 683–688.
[23] S.A. Bashkirov, V.F. Gremenok, V.A. Ivanov, Physical properties of SnS thin films fabricated by hot wall deposition, *J Fizika i Tekhnika Poluprovodnikov* **45-6** (2011), 765–769.
[24] H. Zhu, D. Yang, Y. Ji, H. Zhang and X. Shen, Two-dimensional SnS nanosheets fabricated by a novel hydrothermal method. *J Materials Science* **40** (2005), 591–595.
[25] B. Ghosh, M. Das, P. Banerjee and S. Das, Fabrication and optical properties of SnS thin films by SILAR method, *J Applied Surface Science* **254** (2008), 6436–6440.
[26] B.R. Sankapal, R.S. Mane and C.D. Lokhande, Successive ionic layer adsorption and reaction (SILAR) method for the deposition of large area (10 cm^2) tin disulfide (SnS_2) thin films, *J Materials Research Bulletin* **35** (2000) 2027–2035.
[27] S. Cheng, Y. Chen, Y. He and G. Chen, The structure and properties of SnS thin films prepared by pulse electro-deposition. The structure and properties of SnS thin films prepared by pulse electro-deposition, *J Materials Letters* **61** (2007), 1408–1412.
[28] N. Koteswara Reddy and K.T. Ramakrishna, Reddy, Growth of polycrystalline SnS films by spray pyrolysis, *J Thin Solid Films* **325** (1998), 4–6.
[29] T.H. Sajeesh, A.R. Warrier, C. Sudha Kartha and K.P. Vijayakumar, Optimization of parameters of chemical spray pyrolysis technique to get n and p-type layers of SnS, *J Thin Solid Films*, **518** (2010) 4370–4374.
[30] A. Akkari, M. Reghima, C. Guasch and N. Kamoun, Effect of deposition time on physical properties of nanocrystallized SnS zinc blend thin films grown by chemical bath deposition, *J Mater Sci* **324** (2011) 101.
[31] M. Ajili and M. Castagné, Najoua Kamoun Turki, *Optik* **126** (2015), 708–714.
[32] JCPDS Card No. 23-0677
[33] M. Kul, Electrodeposited SnS film for photovoltaic applications, *J Vacuum* **107** (2014), 213–218.
[34] I.B. Kherchachi, H. Saidi, A. Attaf, N. Attaf, A. Bouhdjar, H. Bendjdidi, Y. Benkhetta, R. Azizi and M. jlassi, Influence of solution flow rate on the properties of SnS_2 films prepared by ultrasonic spray, *J. Optik* **127** (2016), 4043–4046.
[35] N. Koteeswara Reddy and K.T. Ramakrishna Reddy, SnS films for photovoltaic applications: Physical investigations on sprayed Sn_xS_y films, *Physica B* **368** (2005), 5–31.
[36] C. Khelia, K. Boubaker, T. Ben Nasrallah, Mr. Amlouk and S. Belgacem, Morphological and thermal properties of β-SnS_2 sprayed thin films using Boubaker polynomials expansion, *J Alloys and Compounds* **477** (2009), 461–467.
[37] L.L. Cheng, M.H. Liu, S.C. Wang, M.X. Wang, G.D. Wang, Q.Y. Zhou and Z.Q. Chen, *J Semicond Sci Technol* **28** (2013), 015020.
[38] J. Gajendiran and V. Rajendran, *J Adv Nat Sci: Nanosci Nanotechnol* **2** (2011), 015001.
[39] I.B. Kherchachi, A. Attaf, H. Saidi, A. Bouhdjer, H. Bendjedidi, Y. Benkhetta and R. Azizi, Structural, optical and electrical properties of SnxSy thin films grown by spray ultrasonic, *J Semiconductors* **37** (2016), 032001.
[40] S. Biswas, S. Kar and S. Chaudhuri, *Appl Surf Sci* **253** (2007), 9259.
[41] K. Gurumurugan, D. Mangalaraj, S.K. Narayandass, K. Sekar and G. Vallabhan, Characterisation of transparent conducting CDO films deposited by spray pyrolysis. *J Semicond Sci Technol*, **9** (1994), 1827.
[42] B.D. Cullity, Elements of X-ray Diffraction, Addison-Wesley, Reading, MA, (1978) 102.
[43] J.I. Pankove, J. Optical processes in semiconductors; Dover, New York, 1975.
[44] M. Dhanam, P.K. Manoj, R. Prabhu and J. Cryst. *Growth* **280** (2005), 425.
[45] P. Prathap, G. Gowri Devi, Y.P.V. Subbaiah, K.T. Ramakrishna Reddy and V. Ganesan, *J Curr Appl Phys* **8** (2008), 120.
[46] L.L. Cheng, M.H. Liu, M.X. Wang, S.C. Wang, G.D, Wang, Q.Y, Zhou and Z.Q. Chen, *J Alloys and Compounds* **545** (2012), 122–129.
[47] G.B. Williamson, R.C. Smallman, *J Philos Mag* **1**(34e) (1956), 46.
[48] S. Velumani, K. Narayandass, D. Mangalaraj and J. Semicond, *Sci Technol* **13** (1998) 1016–1024.
[49] S. Benramache, B. Benhaoua and O. Belahssen, The crystalline structure, conductivity and optical properties of Co-doped ZnO thin films, *J Optik* **125** (2014), 5864–5868.
[50] N.G. Deshpande, A.A. Sagade, Y.G. Gudage and C.D. Lokhande, Growth and characterization of tin disulfide (SnS_2) thin film deposited by successive ionic layer adsorption and reaction (SILAR) technique, *J Alloy Compd* **436** (2007), 421–426.
[51] O. Parasyuk, I.D. Olekseyuk, L.V. Piskach, S.V. Volkov and V.I. Pekhnyo, *J Alloys Compd* **399** (2005), 173–177.
[52] V. Robles, J.F. Trigo, C. Guillen and J. Herrero, *J Mater Sci* **48** (2013), 3943–3949.
[53] R. Miles, O. Ogah, G. Zoppi and I. Forbes, Thin films of tin sulphide for use in thin film solar cell devices. *Thin Solid Films J Thin Solid Films* **517** (2009), 4702.

[54] H. Moualkia, S. Hariech, M.S. Aida, N. Attaf and E.L. Laifa, *J Phys D: Appl Phys* **42** (2009), 135404.
[55] E. Guneri, C. Ulutas, F. Kirmizigul, G. Altindemir, F. Gode and C. Gumus, Effect of deposition time on structural, electrical and optical properties of SnS thin films deposited by chemical bath deposition. *J Appl Surf Sci* **257** (2010), 1189.
[56] J.H. Lee and B.O. Park, *J Surface and Coatings Technology* **184** (2004), 102–107.